INTERNAL LEAKAGE IN THE MAIN STAGE OF SERVOVALVES: AN ANALYTICAL AND CFD ANALYSIS

Paolo Tamburrano[1,2, a)], Andrew R. Plummer[2)], Phil Elliott[3)], Pietro De Palma[1)], Elia Distaso[1)] and Riccardo Amirante[1)]

[1] *Department of Mechanics, Mathematics and Management (DMMM), Polytechnic University of Bari, Bari, Italy*
[2]*Centre for Power Transmission and Motion control (PTMC), University of Bath, Bath, UK*
[3] *Moog Controls Ltd, Aircraft Group, Tewkesbury, UK*
[a)]Corresponding author: paolo.tamburrano@poliba.it

Abstract. The internal leakage in two stage servovalves causes unwanted power consumption; it is the sum of two contributions: the internal leakage in the main stage and the internal leakage in the pilot stage. While the latter can be assumed almost constant regardless of the spool position, the former is maximum at null and decreases with increasing opening degree of a given valve. Because of this, the power consumption is significant when a valve is at rest, namely, when it is not modulating flow. Despite being a very important feature of these valves, the internal leakage occurring in the main stage around null and its associated issues are not properly addressed in the scientific literature. Because of this, this paper aims at providing a deep investigation into this phenomenon. In particular, it will be discussed how it can be studied using analytical equations. In addition, a CFD analysis is carried out in this paper in order to obtain a simple CFD model that has general validity and that can be used to predict the internal leakage around null in the main stage. The developed model can be easily reproduced by manufacturers, and it can be used to understand the effects of geometrical imperfections and tolerances as well as fluid properties upon the internal leakage around null. The present paper has been realized in collaboration with Moog controls ltd, a world leading manufacturer of servovalves.

INTRODUCTION

In this introductory section, at first the internal leakage occurring in the main stage of servovalves will be explained thoroughly. Simple analytical models will be used to give an insight into this phenomenon, in order to comprehend how the internal leakage is generated through a common spool valve. These analytical equations can also be useful to have an initial estimation of the leakage flow in the main stage of servovalves. However, these models are not capable of taking into account real phenomena, such as imperfections and tolerances. To address these issues, advanced analytical models and CFD models have been developed in the scientific literature; these will be discussed in the second part of the introductory section.

Internal leakage in servovalves studied by simple analytical models

Two-stage servovalves are widely used components in high-dynamic closed-loop hydraulic circuits because of their high-speed frequency response and reliability. They are composed of a main stage (also called second stage) employing a sliding spool inside a bushing sleeve, and a pilot stage (also called first stage) which acts as hydraulic amplifier for the main stage. The pilot stage is always actuated by a torque motor, while the hydraulic amplification

is obtained through a double-flapper nozzle, a deflector jet or a jet pipe. There can be either a mechanical feedback or an electrical one depending on the application (mechanical feedbacks are more used in aircraft) [1-4].

The main stage of a servovalve, because of the clearance existing between the spool and its bushing sleeve, has leakage flow passing from the supply line to the return line. This leakage flow is usually referred to as the leakage of the second stage (or main stage), here denoted by $Q_{leak,II}$. In addition to this, part of the flow coming from the supply line is used by the first stage (or pilot stage), which requires a certain amount of flow to operate. This additional leakage flow is usually referred to as the leakage of the first stage or tare leakage, here denoted by $Q_{leak,I}$. Therefore, the overall leakage through a servovalve is the sum of the two contributions: $Q_{leak} = Q_{leak,I} + Q_{leak,II}$.

To better explain the leakage in the main stage of a servovalve, Fig. 1 (a) shows a drawing of a spool moving inside a bushing sleeve of a generic four way-three position (4/3) valve. Simplified schematizations similar to that shown in Fig.1 have been used by some authors to study the internal leakage in spool valves [5-10]. In Fig. 1(a), the spool is in a generic position *x* (measured from the null position) which determines flow from the high-pressure port P to the actuator port A and from the actuator port B to the tank (P→A and B→T). The supply line delivers a flow rate Q_p at the high pressure P_p. A great part of Q_p enters the valve through the metering section 1 on the left-hand side of Fig.1 (a) (this flow rate is denoted by Q_1 in Fig.1). However, because of the clearance existing between the spool and the bushing sleeve, a small part of the flow Q_p (here denoted by Q_2) enters the valve through clearance 2, shown on the right-hand side of Fig.1 (a). In addition, another small part of Q_p is used by the first stage ($Q_{leak,I}$). Thus, the overall flow coming from the supply line is the sum of the three contributions Q_1, Q_2, and $Q_{leak,I}$:

$$Q_P = Q_1 + Q_2 + Q_{leak,I} \tag{1}$$

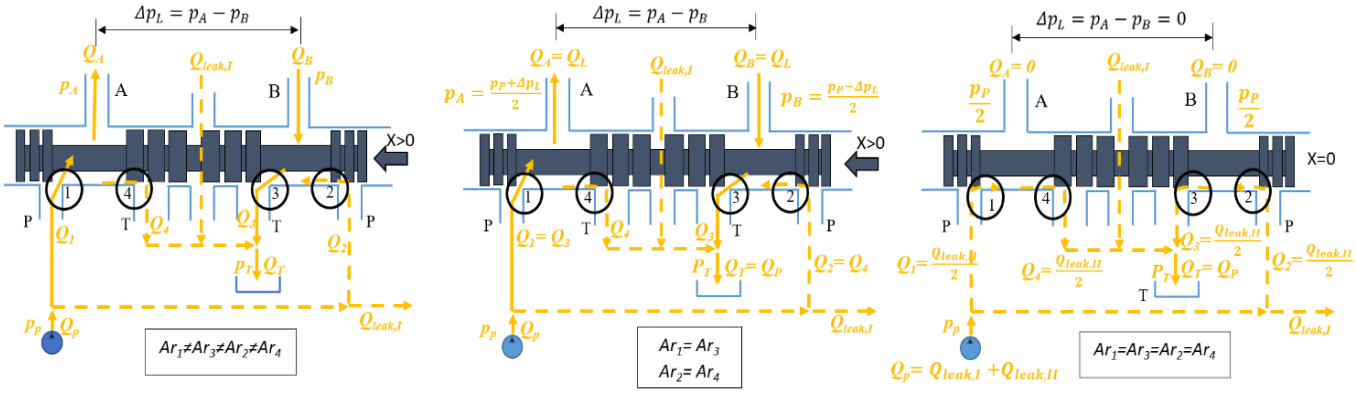

(a) (b) (c)

FIGURE 1. Schematization of a spool inside a bushing sleeve: generic valve with a spool displacement *x* (a), symmetrical valve with a spool displacement *x* (b), symmetrical valve with the spool at null and zero pressure load across the actuator (c)

With regard to the flow sent to the actuator, namely Q_A, its value is slightly lower than Q_1, because a small part of Q_1 (denoted by Q_4) escapes the valve through clearance 4, present between the spool and the bushing sleeve at the left center of Fig.1. Similarly, the flow across metering section 3 (here denoted by Q_3) is the sum of the flow returning from the actuator (Q_B) and the leakage flow coming from the high-pressure line and passing through clearance 2 shown at the right hand side of Fig.1(a) (namely, Q_2). Summarizing, we can write:

$$Q_A = Q_1 - Q_4 \tag{2}$$

$$Q_B = Q_3 - Q_2 \tag{3}$$

The overall flow conveyed to the reservoir, Q_T, is the sum of Q_3, Q_4 and $Q_{leak,I}$:

$$Q_T = Q_3 + Q_4 + Q_{leak,I} \tag{4}$$

Combining equations 1-4 yields:

$$Q_P = Q_T + Q_A - Q_B \tag{5}$$

The overall leakage of the second stage, namely the flow passing directly from the high pressure port P to the reservoir T, is given by the sum of Q_2 and Q_4:

$$Q_{leak,II} = Q_2 + Q_4 \tag{6}$$

The flow rates can be calculated by using the orifice equation, as follows:

$$Q_1 = C_{D,1}A_{r,1}\sqrt{\frac{2(p_P - p_A)}{\rho}} \tag{7}$$

$$Q_2 = C_{D,2}A_{r,2}\sqrt{\frac{2(p_P - p_B)}{\rho}} \tag{8}$$

$$Q_3 = C_{D,3}A_{r,3}\sqrt{\frac{2(p_B - p_T)}{\rho}} \tag{9}$$

$$Q_4 = C_{D,4}A_{r,4}\sqrt{\frac{2(p_A - p_T)}{\rho}} \tag{10}$$

Where C_D denotes the discharge coefficient, A_r the restricted area, and subscripts *1,2,3,4* denote the corresponding restricted sections shown in Fig.1 (a).

The above equations (1-10) can be applied to study the internal leakage trough a generic servovalve. In addition, an assumption that can be made to simplify this study is to consider the valve characteristics to be symmetrical, namely with the symmetrical and matched orifices. Another assumption which can be made is to consider the discharge coefficients symmetrical, thus giving: $C_{D,1}A_{r,1}$=$C_{D,3}A_{r,3}$; $C_{D,4}A_{r,4}$=$C_{D,2}A_{r,2}$. Moreover, the flow rates to and from the actuator are equal in most cases (e.g., due to equal areas of the piston, or when the actuator is a hydraulic motor), thus giving $Q_A = Q_B = Q_L$. This situation is represented in Fig. 1 (b). In this case (symmetric valve with opening degree x≠0), the following relations are obtained:

$$Q_1 = Q_3 \tag{11}$$

$$Q_2 = Q_4 \tag{12}$$

$$Q_P = Q_T \tag{13}$$

Substituting equations 7 and 9 into equation 11 yields:

$$p_P - p_A = p_B - p_T \tag{14}$$

Equation 14 states that the pressure drops across the two metering sections are equal. The pressure drop across the load is Δp_L=$p_A - p_B$; combining the definition of Δp_L with equation (14) yields:

$$p_A = \frac{p_P + p_T + \Delta p_L}{2} \tag{15}$$

$$p_B = \frac{p_P + p_T - \Delta p_L}{2} \tag{16}$$

If the pressure drop across the load Δp_L is zero, and assuming p_T=0 bar, the pressures across the actuator are: $p_A = p_B = \frac{p_P}{2}$. Therefore, it has been demonstrated that, when the spool is moved from its neutral position, in the case of a matched and symmetrical valve connected to a synchronous cylinder ($Q_A = Q_B = Q_L$), the pressure in one line increases as the pressure in the other line decreases by the same amount, corresponding to one half of the pressure drop across the load [5]. If the pressure drop across the load is zero, the pressure in each port is one half of the supply pressure.

A particular case is when the spool is at null. Fig. 1(c) schematizes this case, with the assumption that there is no load across the actuator: $\Delta p_L = p_A - p_B = 0$, namely $p_A = p_B$. Assuming that the valve is symmetrical results in the discharge coefficients being equal, thus giving: $C_{D,1}A_{r,1}$=$C_{D,3}A_{r,3} = C_{D,4}A_{r,4}$=$C_{D,2}A_{r,2}$.Using equations 11-16 leads to $p_A = p_B = p_P/2$, $Q_A = Q_B = Q_L$=0 and $Q_1 = Q_2 = Q_3 = Q_4 = Q_{leak,II}/2$. So, in this case, there is no flow through the actuator and the flow through the main stage is only due to the leakage, which is split into two equal parts. So, in this case, the flow rate delivered by the pump (equal to the flow discharged to the tank) corresponds to the overall leakage through the valve: $Q_P = Q_T = Q_{leak,I} + Q_{leak,II}$.

A typical test carried out to evaluate the effects of leakage upon the valve performance is performed by blocking the control ports with two pressure transducers and moving the spool from the null position to the left and to the right. This test allows measuring the flow rate delivered by the pump or returning to the tank (in this test these flow rates are equal). Therefore, the leakage flow as a function of the input current is retrieved; Fig.2 shows a typical diagram obtained. As mentioned earlier, the leakage flow Q_{leak} is given by the sum of the leakage in the first stage ($Q_{leak,I}$) and the leakage in the second stage ($Q_{leak,II}$). As shown in Fig. 2, it is noteworthy that the first stage leakage is almost constant regardless of the spool position, while the second stage leakage is maximum around null and decreases with the increasing spool displacement. The maximum value of $Q_{leak,II}$, registered at null, is usually denoted by the term center flow, Q_c. The center flow can be analytically predicted by using the schematization of Fig. 1 (c) along with the equations presented above. The main problem arising from this analytical procedure is that the discharge coefficients (equations 7-10) are not known in advance; therefore, an overestimation or underestimation of these coefficients could lead to large errors in the evaluation of the leakage flow.

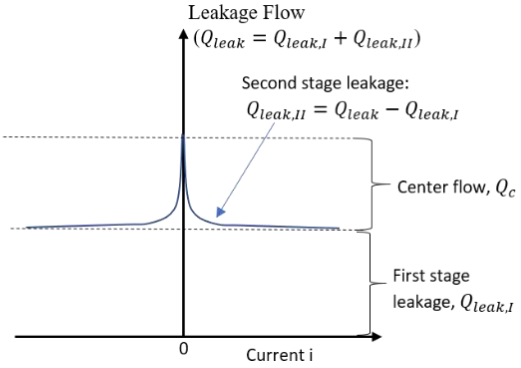

FIGURE 2. Typical leakage flow curve obtained from a test with control ports blocked: leakage flow vs input current

Literature review: advanced analytical models and CFD modelling

Merritt proposed an analytical expression to evaluate the discharge coefficients in equations 7-10 and hence the center flow; this equation, which assumes that the flow is laminar and that the edges of both the spool and the bushing sleeve are sharp [5], is:

$$Q_i = \frac{\pi c^2 w}{32\mu} \Delta p \tag{17}$$

where Q_i is the flow rate through a restriction (*i=1,2,3,4*) and Δp is the corresponding pressure drop, *c* is the clearance between spool and bushing, *w* is the slot width, and μ is the dynamic viscosity. Using equation (17) for a symmetrical 4/3 valve, the center flow becomes: $Q_c = \frac{\pi c^2 w}{32\mu}(p_p - p_T)$. Equation (17) was improved in [6] to take into account the micro-radius on the spool and bushing sleeve edges as a result of manufacturing processes and wear, as follows:

$$Q_i = \frac{\pi l^2 w}{32\mu} \Delta p \tag{18}$$

The parameter *l* in equation 18 can be calculated through a simple geometric relation as a function of the edge radius *r* and clearance *c* [6]:

$$r = \frac{(l-c) + \sqrt{2l(l-c)}}{2} \tag{19}$$

However, equations 17-19 assume that the flow is laminar and neglect the overlap between spool and bushing sleeve. In addition, geometrical imperfections, in addition to increasing the flow area, can also make the flow turbulent. For these reasons, the expressions proposed in [5, 6] might be inaccurate for real valves. In this regard, numerical models have been developed in the scientific literature to evaluate the values of Q_c as a function of geometrical imperfections (radii on the spool and bushing sleeve edges), clearances and overlaps between the spool and its bushing sleeve [7-11]. These are mainly semi-empirical models which require experimental data to be applied to existing valves. An extensive review of these numerical models and their comparison is provided in [7]. The results of these analytical models are also compared with available experimental results. This comparison shows that, on the whole, non-

negligible errors are obtained using those analytical models. This is due to the fact that it is very difficult to evaluate, through analytical models, the effects of the edge conditions upon the internal leakage. Instead, the use of CFD analyses can be instrumental in obtaining accurate predictions of the internal leakage, assessing the effects of real edge conditions, such as the presence of round radii on the edges and the presence of clearance and overlap between the spool and the bushing sleeve. Some papers present in the scientific literature prove that the use of CFD to study the internal leakage is highly viable.

In [12], a partial 3D model was used to predict the discharge coefficients in the metering sections of a 4/3 spool valve. The model also took into account the leakage flow due to the clearance existing between spool and bushing sleeve. However, geometrical imperfections were not considered in that analysis. In [13], the effects of different radii on the spool edge of an existing servovalve were analyzed in detail using a partial 3D model. The results of the numerical predictions show that the presence of a radius on the spool edge has a great effect on the internal leakage. However, the edge of the bushing sleeve was considered sharp and the clearance which normally exists between the spool and the bushing sleeve was not taken into account. Some other papers present in the scientific literature have tried to predict the erosion rate on the spool edges because of contamination particles in order to predict the change in the discharge coefficients of spool valves [6, 14].

All the above-mentioned CFD models have proved to be effective in the evaluation of the flow rate through the metering sections of spool valves. The reliability of CFD in the evaluation of the flow rate through spool valves is also proved by recent CFD models of the flow field in single-stage proportional valves [15-18].

In this scenario, the present paper aims at developing CFD models which can be instrumental in predicting the effects of geometrical imperfections and tolerances upon the internal leakage in the second stages of servovalves. In the following section, the CFD models developed in the present analysis will be described in detail, and the results achieved with these models will be discussed in the final section.

CFD MODELS

Two computational domains are used in the present analysis to provide a deep investigation into the internal leakage at null in the second stages of servovalves. The first domain is shown in Fig. 3 (a). This 2D domain reproduces a part of the second stage of an existing 4/3 Moog servovalve; specifically, the fluid domain in the left-hand side of Fig. 1 (c) is reproduced. The spool is in the central position (i.e., at null) and, because of the clearance existing between the spool and bushing sleeve (c), leakage flow is generated from port P to port A and from port A to port T. A radius is also present on both the spool edge (r_s) and the bushing sleeve edge (r_b), and an overlap between the spool edge and bushing sleeve edge (Δx) exists both in the metering chamber P-A and in the metering chamber A-T.

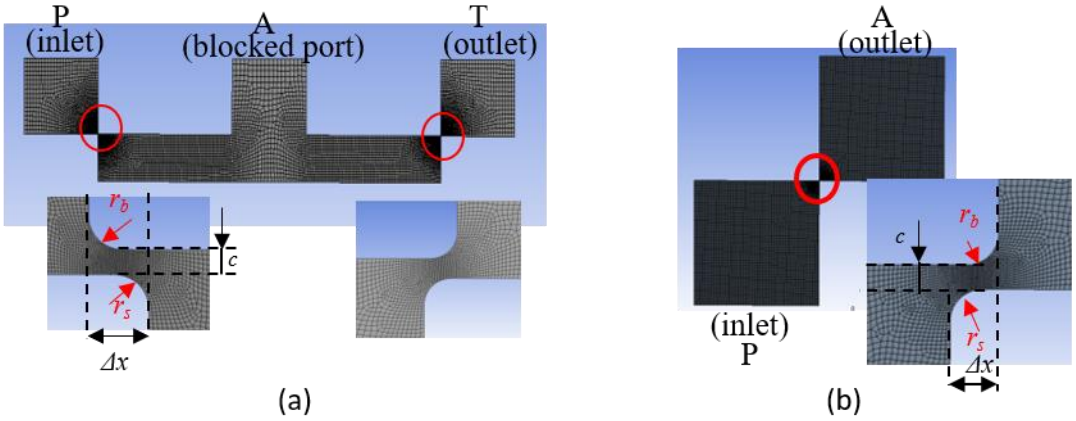

FIGURE 3. 2D computational grids for an existing valve showing the case with radius r_b= r_s=4 μm, clearance c= 3 μm and overlap $\Delta x_{P\text{-}A}$ = 7 μm and $\Delta x_{A\text{-}T}$ = 5 μm (a), and simplified domain showing the case with radius r_b= r_s=4 μm, clearance c= 3 μm and overlap Δx= 6 μm (b)

Fig. 3 (b) shows the second domain considered in this analysis: it is a simplified 2D domain with a dimension of 10 mm for each edge. It reproduces only one metering chamber. Both domains were meshed in Ansys Workbench using unstructured grids; the minimum size of the elements (across the metering section) is 10^{-7} m, with a growth rate of 1.05 and a maximum face size (far from the restrictions) of 10^{-4} m. The corresponding number of cells is 15500 for the grid shown in Fig. 3 (a), and 27000 for the grid shown in Fig. 3 (b). The stationary Reynolds Averaged Navier-

Stokes (RANS) equations were solved in Ansys Fluent using two different settings. The first one is an incompressible single-phase model by which the fluid is treated as incompressible with constant density and viscosity. The second CFD setting employs an incompressible two-phase (mixture) model which is able to predict cavitation when the local pressure decreases down to the vaporization pressure. Among the available cavitation models, the Schnerr and Sauer model was selected, as it is very robust and reliable, as shown by previous studies [15]. In both models, the RNG k-ε model with enhanced wall treatment was implemented to predict turbulence; this choice results from the fact that, using these settings, the flow can be predicted with high accuracy for a wide range of Reynolds number, even in transitional zones [15]. As far as the discretization of the equations is concerned, the second order upwind method was selected for momentum, turbulent kinetic energy and turbulent dissipation rate equations. The selected pressure interpolation scheme is second order accurate for the single-phase model, while the PREssure STaggering Option (PRESTO) was selected for the mixture (cavitation) model. Two-thousand iterations were sufficient to achieve a converged solution, with all the scaled residuals being below 10^{-4}.

RESULTS

In this section, the numerical results obtained with the domain reproducing a part of an existing valve (see Fig. 3 (a)) are shown at first. Two different geometrical conditions are initially considered, as shown in Fig. 4. In the first one, the overlap in the metering section P-A is taken equal to $\Delta x_{P\text{-}A}$ = 7 μm and the overlap in the metering section A-T is taken equal to $\Delta x_{A\text{-}T}$ = 5 μm (these overlaps are often used in Moog servovalves). The clearance is considered equal to c = 3 μm and the radius on the edges is assumed equal to $r_b = r_s$ = 4 μm. The second geometrical condition has the same parameters as far as the clearance and radii are concerned (namely, c = 3 μm and $r_b = r_s$ = 4 μm), but the overlap in the metering section P-A is the same as the overlap in the metering section A-T; specifically, the overlap is taken equal to the average of the two overlaps considered in the other geometrical condition, namely $\Delta x_{P\text{-}A} = \Delta x_{A\text{-}T}$ = 6 μm. In both cases, the inlet pressure was set to p_A=210 bar and the discharge pressure was set to p_T = 1 bar (these are values commonly used to describe a performance of a valve, such as the Bode plot). The property of Hyjet at 40 °C were used for the density (ρ) and viscosity (μ) of the liquid, namely ρ=985 kg/m^3 and μ=0.01 kg/(ms).

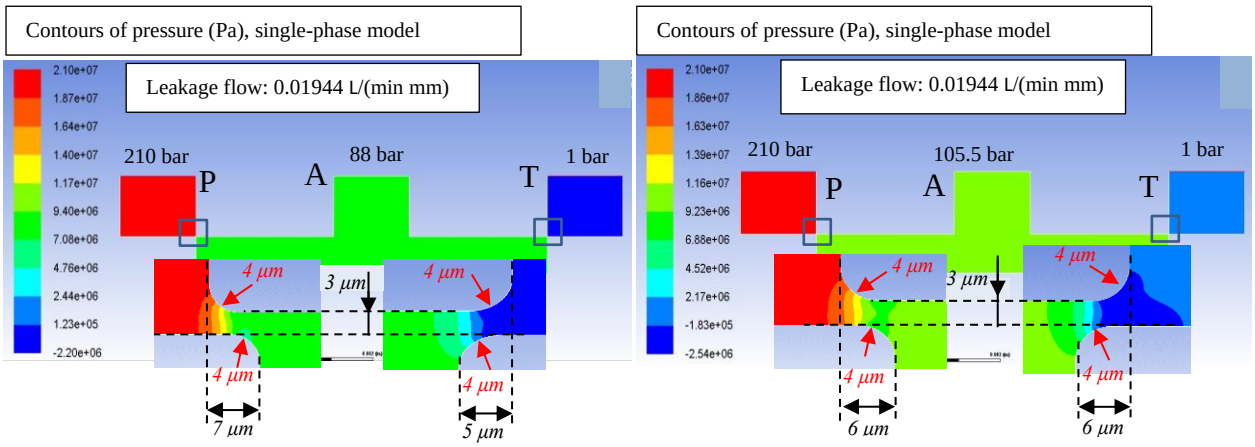

FIGURE 4. Contours of pressure for a valve with 210 bar inlet pressure and 1 bar outlet pressure (ρ=985 kg/m^3 and μ=0.01 kg/(ms)); (a): $\Delta x_{P\text{-}A}$ = 7 μm, $\Delta x_{A\text{-}T}$ = 5 μm, c = 3 μm, $r_b = r_s$ = 4 μm; (b): $\Delta x_{P\text{-}A} = \Delta x_{A\text{-}T}$ = 6 μm , c = 3 μm, $r_b = r_s$ = 4 μm.

The comparison between the two cases of Fig.4 reveals that the pressure distributions are different. Specifically, the pressure at port A is lower for the case of Fig. 4 (a); this can be attributed to fact that the overlaps in Fig. 4 (a) are not symmetrical, thus causing different pressure drops between chamber P-A and chamber A-T. Instead, in the case of Fig. 4 (b), the pressure drop is equally split between chamber P-A and chamber A-T, because of the geometrical symmetry. Thus, the numerical predictions have confirmed what was previously explained from an analytical point of view; namely, for a symmetrical valve at null and without load across the actuator, the pressure drop is equally split between the metering chambers, and the pressure at port A becomes a half of the overall pressure drop. However, in spite of the different pressure distributions, the numerical prediction of the flow rate (i.e., leakage flow) is the same in the two cases of Fig. 4, namely 0.01944 L/(min mm). This is a significant result, because it suggests that, as far as the

leakage flow is concerned, a non-symmetrical valve can be treated as a symmetrical valve having equal overlaps at chambers P-A and B-T, provided that these overlaps are equal to the average of the two different overlaps of the non-symmetrical valve.

The two cases of Fig. 4 were obtained by considering an equal radius for the spool edge and the bushing sleeve edge. In order to understand the effects of different radii on the spool and bushing sleeve edges, Fig. 5 (a) shows the contours of pressure obtained for $\Delta x_{P\text{-}A}$ = 7 μm, $\Delta x_{A\text{-}T}$ = 5 μm, c = 3 μm, r_b =5 μm and r_s = 3 μm; instead, Fig. 5 (b) shows the contours of pressure obtained for $\Delta x_{P\text{-}A}$ = 7 μm, $\Delta x_{A\text{-}T}$ = 5 μm , c = 3 μm, , r_b =6 μm and r_s = 2 μm. Again, in both cases, the inlet pressure was set to p_A=210 bar and the discharge pressure was set to p_T = 1 bar, with ρ=985 kg/m^3 and μ=0.01 kg/(ms). These two further cases have the same geometrical conditions as those of the case of Fig. 4 (a), apart from the radii on the edges, with the radii on the bushing sleeve being higher than the radii on the spool. The average of the two radii is, in both cases of Fig. 5 (a) and Fig. 5 (b), equal to the radius considered in the cases of Fig. 4 (a) and Fig. 4 (b), namely 4 μm. The contours of pressure in Fig. 5 (a) and Fig. 5 (b) reveal that the different radii cause different pressure drops between chamber P-A and chamber A-T; however, in terms of flow rate, the difference between the cases of Fig. 5 and Fig.4 is less than 1%.

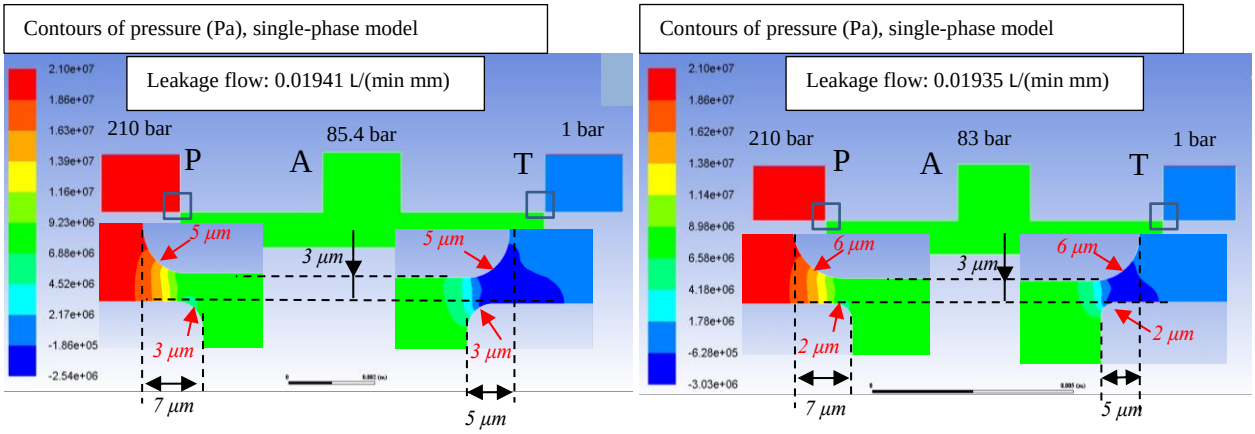

(a) (b)

FIGURE 5. Contours of pressure for a valve with 210 bar inlet pressure and 1 bar outlet pressure (ρ=985 kg/m^3 and μ=0.01 kg/(ms)); (a): $\Delta x_{P\text{-}A}$ = 7 μm, $\Delta x_{A\text{-}T}$ = 5 μm, c = 3 μm, r_b =5 μm and r_s = 3 μm; (b): $\Delta x_{P\text{-}A}$ = 7 μm, $\Delta x_{A\text{-}T}$ = 5 μm , c = 3 μm, r_b =6 μm and r_s = 2 μm.

Summarizing, the numerical results analyzed so far have shown that, in order to evaluate the internal leakage, a non-symmetrical valve with different overlaps and different radii on the edges can be treated as a symmetrical valve having an equal radius on the edges of both the spool and bushing sleeve, provided that the overlap and the radius are taken equal, respectively, to the average of the overlaps and to the average of the radii of the non-symmetrical valve.

A further consideration can be deduced from the contours of pressure shown in Fig. 4 and Fig.5. Specifically, it is evident that large pressure variations are located across the narrow zones of the metering sections, whilst all the other zones of the domain do not experience appreciable pressure variations. It can be concluded that there is no need to simulate a valve with specific dimensions, but only the characteristics of the narrow flow passages are needed, namely, the values of the clearance (c), radii on the spool and bushing sleeve edges (r_b , r_s), and overlap (Δx). Therefore, instead of using a full domain, a simplified domain as that proposed in Fig. 3 (b) can be used to predict the leakage.

As a confirmation of the feasibility of using the simplified 2D domain, Fig. 6 (a) shows the contours of pressure predicted by the single-phase model on the simplified domain for an inlet pressure of 105.5 bar, namely, for an inlet pressure which is equal to a half of the overall pressure drop P-T previously considered, and for an outlet pressure of 1 bar. To allow the comparison, the same geometrical conditions as those of Fig. 4 (a) are considered, namely the same average overlap Δx = 6 μm, the same clearance c = 3 μm, and the same edge radius r =4 μm, with ρ=985 kg/m^3 and μ=0.01 kg/ms. As shown by the pressure contours, the numerical predictions are very similar in the two cases of Fig. 4 (a) and Fig. 6(a), which results in a very similar flow leakage (0.01944 L/(min mm) vs 0.01943 L/(min mm)), with the percentage difference being below 1‰. Therefore, it has been demonstrated that the leakage flow of both a non-symmetrical valve and a symmetrical valve can be predicted by the simplified domain shown in Fig. 3b, provided that the pressure drop is taken equal to a half of the overall pressure drop of the entire valve.

In all the simulations performed with the single-phase model, negative pressures have been predicted, as shown by the contours of pressure of Figures 4 to 6(a). This is due to the fact that the single-phase model is not capable of simulating the phase change (cavitation) when the pressure decreases down to the vaporization pressure. In order to properly predict this phenomenon, the mixture model was used; the presence of non-condensable gases in the liquid, which can increase the volumes of the vapor cavities, was taken into account by assuming the properties of the vapor phase equal to those of air, namely ρ=1.225 kg/m^3 and μ=1.7894e^{-05} kg/(ms). In this regard, Fig. 6 (b) shows the contours of pressure predicted by the mixture model on the simplified domain for an inlet pressure of 105.5 bar and an outlet pressure of 1 bar, with ρ=985 kg/m^3 and μ=0.01 kg/ms. Also in this case, the radii on the spool and bushing sleeve edges are taken equal to *4* μm, the clearance is assumed equal to *3* μm, and the overlap is set to *6* μm. The contours of pressure in Fig. 6 (b) show that the negative pressures have disappeared. Similarly, Fig. 7 shows the comparison, in terms of contours of velocity, between the single-phase model (Fig. 7 (a)) and the mixture model (Fig. 7 (b)), both of them applied to the simplified domain with the same geometrical and boundary conditions as those of Fig.6. The comparison between the velocity contours of Fig. 7 (a) and Fig. 7 (b) show that these are very similar in the two cases, which results in a very similar flow rate (leakage flow) predicted in the two cases. In fact, the flow rate predicted with the single-phase model is 0.01943 L/(min mm), whereas the flow rate predicted with the mixture model is 0.01922 L/(min mm), with a percentage difference of about 1%. Therefore, it can be concluded that, although cavitation is present in the fluid domain, the effects in terms of flow rate are negligible, therefore the simplified domain with the single-phase model can be used to obtain accurate predictions of the leakage flow.

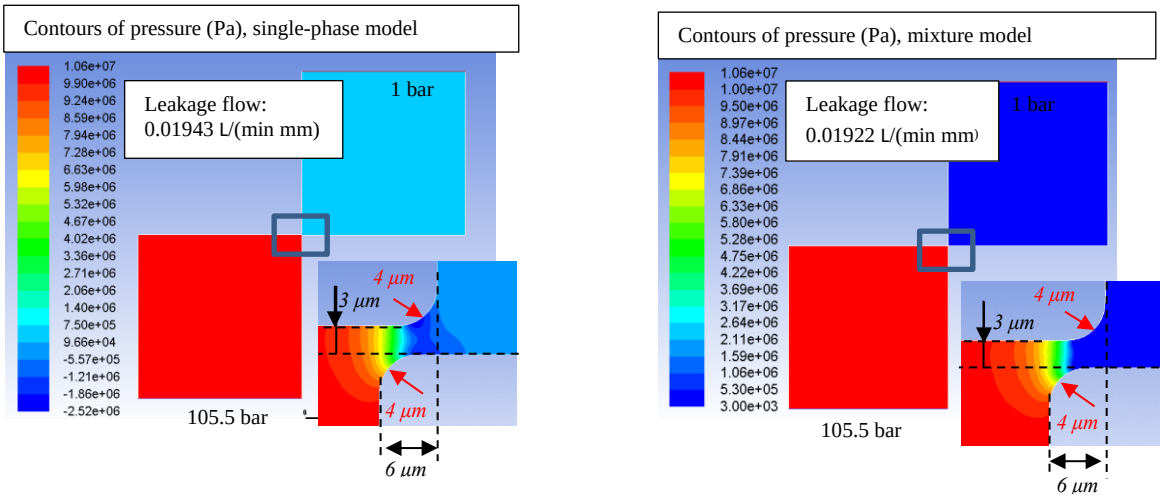

(a) (b)

FIGURE 6. Contours of pressure for the simplified domain with 105.5 bar inlet pressure and 1 bar outlet pressure, Δx = 6 μm, c = 3 μm, r_b = r_s = 4 μm (ρ=985 kg/m^3 and μ=0.01 kg/(ms)); single-phase model (a) and mixture model (b)

This model can be used to assess the effects of the geometrical tolerances (clearance c and overlap Δx) and geometrical imperfections upon the internal leakage. As an example, Fig. 8 (a) and Fig. 8 (b) show the contours of velocity predicted with the same boundary conditions and the same geometrical conditions as those of Fig. 7, apart from the edge radius, which is taken equal to 6 μm (Fig. 8 (a)) and 10 μm (Fig. 8 (b)). The comparison among Fig. 7 (a), Fig. 8 (a) and Fig. 8 (b) reveals that the increase in the radius causes an increase in the maximum velocity across the narrow section (from 141 m/s in Fig. 7 (a) to 161 m/s in Fig. 9 (b)). Correspondingly, the increase in the velocity plus the increase in the flow area determine a large increase in the leakage flow, which results to be 0.01943 L/(min mm) for a radius of 4 μm, 0.025974 L/(min mm) for a radius of 6 μm, and 0.05186 L/(min mm) for a radius of 10 μm.

As a conclusion, Table (1) shows the difference between the numerical predictions obtained with the single-phase model and the analytical predictions obtained both through equation (17), and through equations (18) and (19). To allow the comparison, the overlap was considered equal to zero; the clearance was taken equal to 3 μm, the inlet and outlet pressures were taken equal to 70 bar and 1 bar. Different radii were considered for this comparison, i.e., 2 μm, 4 μm, and 6 μm (note that the radius is not taken into account by equation 17). As shown by the comparison, large errors are obtained through the analytical models, ascribable to the fact that they are valid only for laminar flows and are not able to take into account real phenomena, such as the formation of the vena contracta in the flow path.

The 2 D model developed in this paper will be used in the second part of this paper [19] to provide more results of leakage flow as a function of the overlap, radius and clearance. A comparison with experimental data will also be given to validate the numerical model developed in this paper.

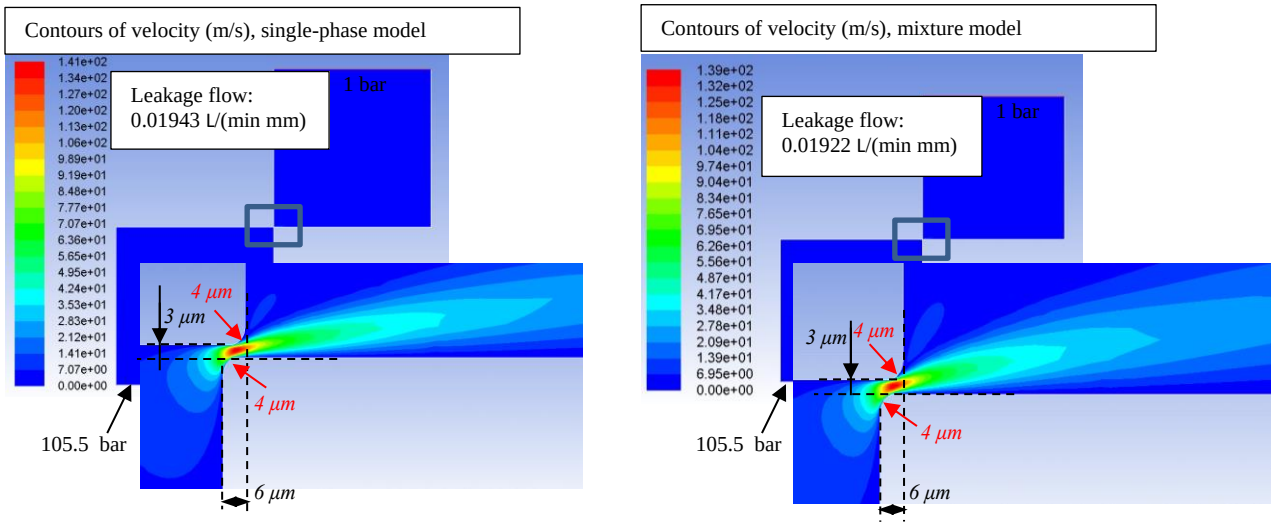

(a) (b)

FIGURE 7. Contours of velocity for the simplified domain with 105.5 bar inlet pressure and 1 bar outlet pressure, Δx = 6 μm, c = 3 μm, r_b = r_s = 4 μm (ρ=985 kg/m^3 and μ=0.01 kg/(ms)); single-phase model (a) and mixture model (b)

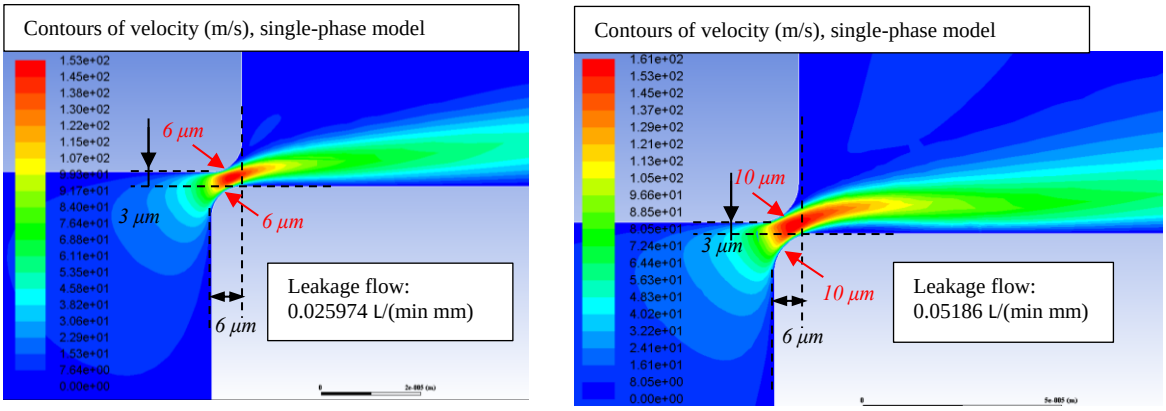

(a) (b)

FIGURE 8. Contours of velocity for the simplified domain with 105.5 bar inlet pressure and 1 bar outlet pressure, Δx = 6 μm, c = 3 μm, (ρ=985 kg/m^3 and μ=0.01 kg/(ms)); r_b = r_s = 6 μm (a) and r_b = r_s = 10 μm (b)

TABLE 1. Comparison in terms of flow rate between CFD (single-phase, simplified domain) and analytical predictions

70 bar inlet pressure, 1 bar outlet pressure (c=3 μm, overlap=0)	**CFD prediction l/(min mm)**	**Analytical prediction eq.17 l/(min mm)**	**Analytical prediction eq.18 and eq. 19 l/(min mm)**
r_b = r_s = 2 μm	0.02311	0.03658	0.0670
r_b = r_s = 4 μm	0.03355	0.03658	0.1275
r_b = r_s = 6 μm	0.04416	0.03658	0.2112

CONCLUSIONS

This paper provided a thorough explanation of the internal leakage occurring around null in the main stages of servovalves. The internal leakage is a major feature of these valves: in some applications it is needed for cooling, but it also causes unwanted power consumptions. At first, the paper discussed simple analytical models which can be used

to study the internal leakage around null; it was also discussed in the paper how these equations have been improved in the scientific literature in order to account for geometrical imperfections and tolerances which exist in real valves. However, it seems that the only way to have reliable predictions is to use CFD; so far, in the scientific literature there are not CFD models having general validity and capable of taking into account all the geometrical tolerances (overlaps and clearances) and imperfections (radii on the edges). For these reasons, this paper has been focused on the development of a simple CFD model which can be applied to different servovalves. Two computational domains were used in the present analysis. The first domain reproduces a part of the second stage of an existing 4/3 Moog servovalve. Using this domain, it was shown that a non-symmetrical valve can be treated as a symmetrical valve having average values for the overlaps and for the radii on the edges. In addition, it was shown that, since the pressure variations are located across the narrow zones of the metering sections, there is no need to simulate a valve with specific dimensions, but only the characteristics of the narrow flow passages are needed. For these reasons, a simplified domain was proposed to be used, and it was demonstrated that the leakage flow around null of both a non-symmetrical valve and a symmetrical valve can be predicted using this simplified domain, provided that the pressure drop is taken equal to a half of the overall pressure drop of the entire valve. To obtain the leakage flow through a real valve, the flow rate predicted in the plane must be multiplied by the slot width and the number of slots of the given valve.

REFERENCES

1. Plummer, A.R. “Electrohydraulic servovalves – past , present , and future,” 10th Int. Fluid Power Conf., pp. 405–424, 2016.
2. Tamburrano, P., Plummer, A. R., Distaso, E., & Amirante, R. (2018). A review of electro-hydraulic servovalve research and development. International Journal of Fluid Power, 1-23.
3. Tamburrano, P., Amirante, R., Distaso, E., & Plummer, A. R. (2018). Full simulation of a piezoelectric double nozzle flapper pilot valve coupled with a main stage spool valve. Energy Procedia, 148, pp. 487-494
4. Tamburrano, P., Amirante, R., Distaso, E., and Plummer, A.R. (2018). A Novel Piezoelectric Double-Flapper Servovalve Pilot Stage: Operating Principle and Performance Prediction. In Bath/ASME Symposium on Fluid Power and Motion Control FPMC 2018, 12 - 14 September 2018, University of Bath, Bath (UK).
5. Merritt, Herbert, Herbert E. Merritt, and Herbert E. Merritt. Hydraulic control systems. John Wiley & Sons, 1967.
6. Fang, Xin, Jinyong Yao, Xizhong Yin, Xun Chen, and Chunhua Zhang. "Physics-of-failure models of erosion wear in electrohydraulic servovalve, and erosion wear life prediction method." Mechatronics 23, no. 8 (2013): 1202-1214.
7. Gordić, D., M. Babić, D. Milovanović, and S. Savić. "Spool valve leakage behaviour." Archives of Civil and Mechanical Engineering 11, no. 4 (2011): 859-866.
8. Ellman A., Virvalo T: Formation of pressure gain in hydraulic servovalves and its significance in system behavior, Proceedings of the ASME Fluid Power Systems and Technology, Vol. 3, 1996, pp. 77–81.
9. Ellman A. Leakage behaviour of four-way servovalve, Proceedings of the ASME Fluid Power Systems and Technology, Vol. 5, 1998, pp. 163–167
10. Eryilmaz, Bora, and Bruce H. Wilson. "Modeling the internal leakage of hydraulic servovalves." In International Mechanical Engineering Congress and Exposition, ASME, vol. 69, pp. 337-343. 2000.
11. Eryilmaz, Bora, and Bruce H. Wilson. "Combining leakage and orifice flows in a hydraulic servovalve model." Transactions-American Society Of Mechanical Engineers Journal Of Dynamic Systems Measurement And Control 122, no. 3 (2000): 576-579.
12. Di Rito, Gianpietro. "Experiments and CFD simulations for the characterisation of the orifice flow in a four-way servovalve." International Journal of Fluid Power 8, no. 2 (2007): 37-46.
13. Pan, Xu Dong, Guang Lin Wang, and L. Zhang. "Simulation study on spool edge’s round angle effects on spool valve orifice discharge characteristic." In Applied Mechanics and Materials, vol. 10, pp. 918-922. Trans Tech Publications, 2008.
14. Xin Bi, Huang, and Jinyong Yao. "Research to the wear and geometric error relations of electro hydraulic servo valve." Procedia Engineering 15 (2011): 891-896.
15. Amirante, R., Distaso, E., & Tamburrano, P. (2014). Experimental and numerical analysis of cavitation in hydraulic proportional directional valves. Energy Conversion and Management, 87, 208-219.
16. Tamburrano, P., Plummer, A. R., Distaso, E., & Amirante, R. (2018). A review of electro-hydraulic servovalve research and development. International Journal of Fluid Power, 1-23.
17. Amirante, R., Distaso, E., & Tamburrano, P. (2016). Sliding spool design for reducing the actuation forces in direct operated proportional directional valves: Experimental validation. Energy Conversion and Management, 119, pp. 399-410
18. Amirante, R., Catalano, L. A., Poloni, C., & Tamburrano, P. (2014). Fluid-dynamic design optimization of hydraulic proportional directional valves. Engineering Optimization, 46(10), 1295-1314.
19. Tamburrano, P., Plummer, A.R., Elliott, P., Morris, W., Page, S., De Palma, P., Distaso, E., Amirante, R. 2D CFD Analysis of Servovalve Main Stage Internal Leakage. Proceedings of the ASME/BATH 2019 Symposium on Fluid Power and Motion Control FPMC2019, October 7-9, 2019, Sarasota, FL, USA.